minerals

MDPI

Review

A Discussion on CO_2 Sequestration in the UCG Space Based upon the Review of the UCG Residue Physicochemical Properties

Run Chen [1,2,*], Fengrong Lv [1,2], Yunxia Bao [1,2], Fu Chen [3,*], Tianzheng Dou [1,2] and Guanglong Tu [1,2]

[1] Jiangsu Key Laboratory of Coal-Based Greenhouse Gas Control and Utilization, Carbon Neutrality Institute, China University of Mining and Technology, Xuzhou 221008, China
[2] Key Laboratory of Coalbed Methane Resource & Reservoir Formation History, Ministry of Education, School of Resource and Geoscience, China University of Mining and Technology, Xuzhou 221008, China
[3] School of Public Administration, Hohai University, Nanjing 210098, China
* Correspondence: chenrun@cumt.edu.cn (R.C.); chenfu@hhu.edu.cn (F.C.); Tel.: +86-15805203840 (R.C.); +86-13852158818 (F.C.)

Abstract: The strategic goal of "carbon peaking and carbon neutrality" has promoted further reform of the global energy system. Additionally, coal is still the dominate form of energy consumption. Underground coal gasification, which changes the method of coal utilization, is an important way to execute clean coal development and clean utilization, and is also an effective method for the development of deep coal resources, belonging to the technical category of clean energy resources. Compared with the traditional method of coal mining surface gasification, it has obvious advantages of being economical, safe and environmentally friendly. After high-temperature gasification, the physicochemical properties of the residues in the three reaction zones of UCG are significantly different from those of the raw coal. Therefore, this paper summarizes the transformation characteristics and the evolution of organic matter and minerals during UCG. Moreover, the paper analyzes the transformation of pore structure caused by UCG and its influencing mechanism, and discusses the possible utilization of UCG residue based on its physicochemical properties. The results show that: (1) after the UCG, the gasification center residue was mainly composed of acidic and alkaline oxides, accompanied by glassy silica that wrapped the carbon residue, which was located far from the gasification center. Due to the weakening of the oxygen supply, the chemical reaction changed from oxidation to reduction, and the influence of baking on the pyrolysis of coal and minerals gradually weakened. Furthermore, the organic carbon content in the residue gradually increased, whereas the inorganic mineral content decreased. Additionally, the thermal decomposition declined. In the boundary between the dry distillation zone and the raw coal, the organic skeleton of coal and inorganic minerals remained basically unchanged. (2) It is suitable for carbonation to sequestrate CO_2 for the oxidation residue after the oxidation process because the residue was composed of slag, whereas the baked roof rock fell off. It is suitable for high-pressure adsorption to sequestrate CO_2 in the reduction coal due to the porous and high specific surface of the pyrolysis coal. Some pyrolytic minerals were conducive to mineralization to sequestrate CO_2. The dry distillated coal had higher specific surface area and volume of pores in the dry distillation zone than those of the raw coal, whereas the values were lower than those of the reduction zone. The pyrolysis of minerals was not obvious, and the carbonation of CO_2 was relatively low. The study points out that CO_2 sequestration in the UCG space is an important way to reduce greenhouse gas emissions under the dual carbon peak and neutralization targets. The use of UCG cavities for CO_2 sequestration is important for achieving the strategic goal of carbon neutrality. However, the current research on CO_2 sequestration using UCG cavities is at the theoretical stage, further field tests are lacking and the commercialization process of CO_2 sequestration has not yet been realized.

Keywords: UCG residue; physicochemical property; mineral transformation; mineral carbonation; gas adsorption; CO_2 sequestration

check for updates

Citation: Chen, R.; Lv, F.; Bao, Y.; Chen, F.; Dou, T.; Tu, G. A Discussion on CO_2 Sequestration in the UCG Space Based upon the Review of the UCG Residue Physicochemical Properties. *Minerals* **2023**, *13*, 616. https://doi.org/10.3390/min13050616

Academic Editor: Samintha Perera

Received: 2 February 2023
Revised: 21 April 2023
Accepted: 27 April 2023
Published: 28 April 2023

Copyright: © 2023 by the authors. Licensee MDPI, Basel, Switzerland. This article is an open access article distributed under the terms and conditions of the Creative Commons Attribution (CC BY) license (https://creativecommons.org/licenses/by/4.0/).

1. Introduction

With the backdrop of carbon neutrality, the global energy system is facing two major challenges. Firstly, it must meet the continuous growth of energy demand. Secondly, it needs to adapt to the green development of a low-carbon society [1]. China is a country rich in coal, but poor in oil and gas. Therefore, the production and consumption of coal have accounted for a high proportion in China's energy infrastructure for a long time [2–4]. Meanwhile, as the country with the largest energy consumption and the highest total CO_2 emissions in the world, China's demand for oil and gas has increased year after year. Although the proportion of coal consumption has decreased slightly, its CO_2 emissions still account for about 1/4 of the total global emissions [5]. Based upon the fact that this situation endangers the security of national energy, the central government needs "to increase the domestic natural gas exploration and development efforts to ensure that the increase in reserves and production can achieve tangible results" [6]. Even so, due to the factors such as the heterogeneity of China's energy structure, the reliability of obtaining coal resources and the need for their sustainable utilization, the position of coal as the basic energy resource will not change for a long time. Underground coal gasification (UCG) is characterized by low cost, high efficiency, high resource recovery rate, reliable operation and small environmental impact. It is considered as an important method for efficient coal mining and utilization in the context of carbon neutralization.

After the concept and basic technology of UCG were proposed by William Simmons in 1868 and Mendeleev in 1888 [7], respectively, many western countries have carried out exploration and research on the establishment and application of UCG field-experiments for nearly 100 years [7–9]. The Soviet Union began to study UCG projects in 1926, and established five industrial-scale UCG projects, which came in operation during the time period of 1961–1969. Some of them were running even until 2009 [8]. The gasification site, gasification process, monitoring and prevention of pollutants are hotspots in the research of UCG [7,9–11]. Only a handful of studies have focused on the physical and chemical properties of UCG residue and CO_2 sequestration in the UCG space. Therefore, based on previous studies, this paper compares and analyzes the compositions and pore structures of the residues from the oxidation, reduction and dry distillation zones caused by UCG. Moreover, CO_2 sequestration in the UCG space was proposed based on the physical and chemical properties of the UCG space.

2. Distribution of Minerals in Coal and UCG Residue

2.1. Principle of UCG and Its Influence

UCG is mainly obtained by in situ gasification of coal seams, which is achieved by adding the gasification agent to the gasification working face of coal seams through the air flow channel that connects the ground and coal seams, and outputs the combustible gas to the ground [10,11]. Therefore, compared with the ordinary coal gasification technology, there are great differences in temperature, pressure and chemical reaction. According to the differences in the values of coal seam thickness, chemical reaction and gas composition, the UCG space is divided into "three reaction zones", namely the oxidation zone, the reduction zone and the dry distillation zone [12]. The division of "three reaction zones" is presented in Table 1.

Previous studies have shown that coal mainly undergoes oxidation reaction in the oxidation zone. Moreover, there is only a small amount of residual carbon in the slag after UCG, which is mainly characterized by coal's expansion, fragmentation and transformation of its material phase in the reduction zone. Meanwhile, the coal cracks and shrinks in the dry distillation zone, as shown in Figure 1 [7,10–12].

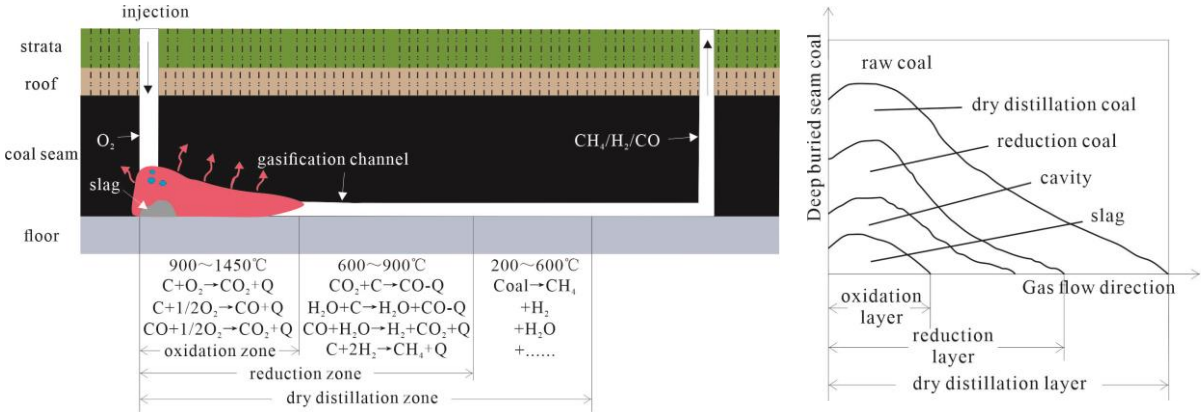

Figure 1. Underground coal gasification principle and the three gasification reaction zones.

Table 1. Division of UCG zones.

Three Reaction Zones	Temperature (°C)	Chemical Reaction	Function
oxidation zone	900–1450	$C + O_2 \rightarrow CO_2$ $2CO + O_2 \rightarrow 2CO_2$	Provide energy for reaction of reduction and dry distillation zones
reduction zone	600–900	$CO_2 + C \rightarrow 2CO$ $H_2O + C \rightarrow CO + H_2$ $CO + H_2O \rightarrow CO_2 + H_2$	CO_2 reduction, steam decomposition and other reactions occur, which are endothermic in nature
dry distillation zone	200–600	$COAL \rightarrow H_2 + CO + CO_2 + CH_4$	Coal seam pyrolysis, drying and dehydration

There are significant differences in the composition of material between the raw coal and the UCG residues from the three reaction zones (see Table 2). The ash content of raw coal was 8.96%, whereas after the UCG, the ash content of the residue in the oxidation zone was 94.9% [13], indicating that carbon combustion mainly occurred in the oxidation zone. Meanwhile, it can be seen that the slag contained a small amount of unburnt carbon in the oxidation zone. The volatile content of the residue in the reduction zone was lower than that of the residue in the dry distillation zone, whereas the content of fixed carbon was slightly higher than that in the dry distillation zone. This was because the UCG coal seam was fixed and the gasification working face moved. Based upon the temperature and the reaction of the coal seam, the coal seam first underwent baking, and then underwent a gasification reaction at higher temperatures, lowering the volatile content of the residue in the reduction zone and increasing the fixed carbon content. The results showed that the residues in the reduction and dry distillation zones contained a small amount of O and S atoms.

Table 2. Proximate and ultimate analysis of the samples (adapted from [13]).

Samples	Proximate Analysis				Ultimate Analysis				
	M_d	A_d	V_{daf}	FC_{daf}	C_{daf}	H_{daf}	O_{daf}	N_{daf}	$S_{t,d}$
Raw coal	1.36	8.96	9.02	90.98	93.26	2.91	2.36	0.35	1.09
Dry distillation residue	-	9.69	4.58	95.42	97.22	0.04	1.16	0.20	0.35
Reduction residue	-	11.04	2.49	97.51	97.52	0.03	1.89	0.2	0.36
Oxidation residue	-	94.90	43.61	56.39	-	-	-	-	-

X-ray diffraction results showed that the residues in the reduction and dry distillation zones have obvious 002 (19–24°) and 100 (42–45°) characteristic peaks of graphite-type carbon (Figure 2) [13]. The Fourier-transform infrared (FTIR) spectra of the residues

from the three reaction zones exhibited the vibration absorption peaks of hydroxyl and C=C (The peak position shifted slightly, and the hydroxyl group of the dry distillation coal, the reduction coal and the oxidized slag from 3420 cm^{-1} of the original coal to 3440 cm^{-1} and the C=C functional group beam changes from 1630 cm^{-1} of the original coal to 1639 cm^{-1}.), whereas the residues from the oxidation zone contained some unburnt carbon (Figure 3) [13].

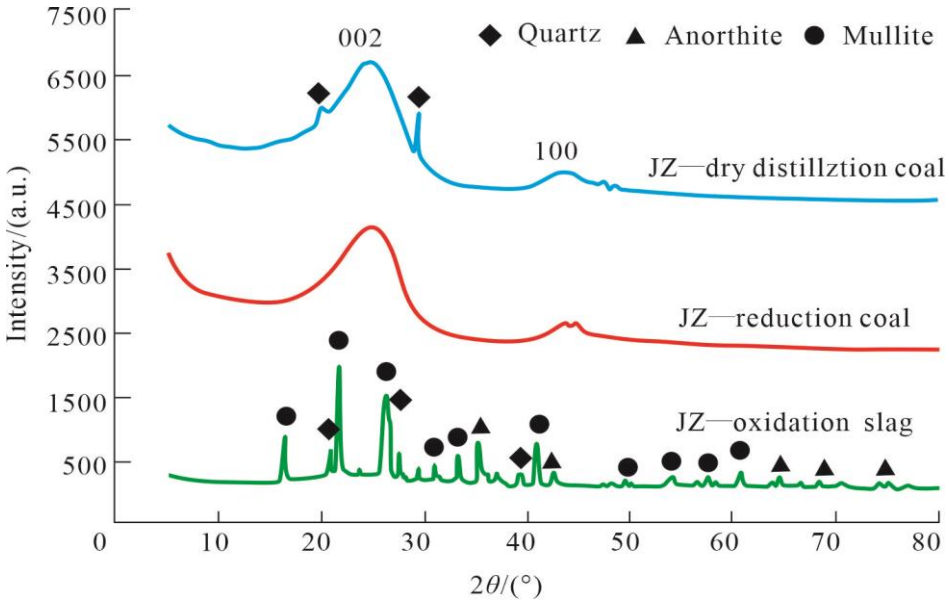

Figure 2. XRD spectra of the samples from three reaction zones (adapted from [13]). JZ—Jiaozuo coal.

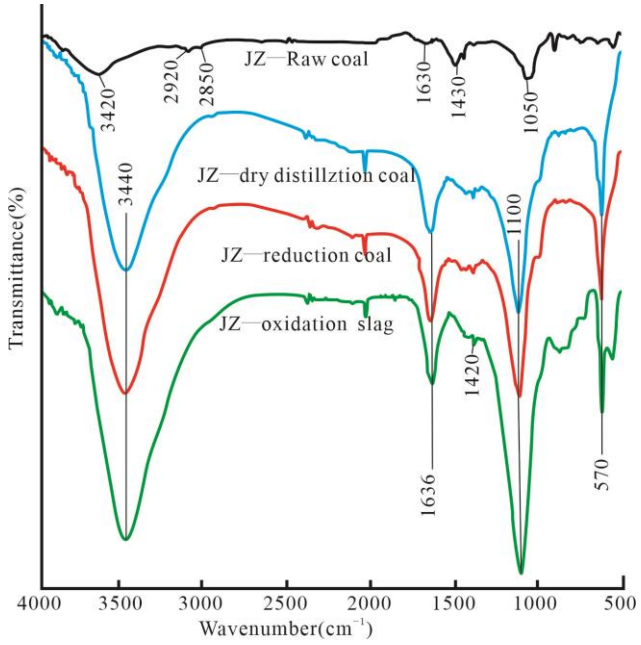

Figure 3. FTIR spectra of the samples from three reaction zones (adapted from [13]). JZ—Jiaozuo coal.

2.2. Minerals in Coal and Its Transformation Due to UCG

2.2.1. Minerals in Coal

Inorganic minerals in coal refer to all components in dry coal that do not contain organic carbon, organic oxygen, organic hydrogen, organic nitrogen or organic sulfur [14]. The minerals in coal can be divided into intrinsic and extrinsic minerals according to the

difference in sources. The intrinsic minerals include primary and secondary minerals. Primary minerals refer to inorganic substances contained in coal and formed due to plants with a mass fraction of only 1%–2%. Secondary minerals are the minerals that enter the coal seam during the formation process of coal, and their mass fraction is less than 10%. Exogenous minerals are the minerals mixed into coal from the roof, floor and the gangue during the mining of coal. Previous studies have shown that the minerals in coal mainly include clay minerals, carbonate minerals, silicate minerals, oxides, sulfide minerals, sulfate minerals and phosphate minerals (see Table 3) [14–18].

Table 3. Composition and mass fraction of main inorganic minerals in coals.

Minerals		Chemical Formula	Mass Fraction	Refs.
clay	kaolinite	$Al_2Si_2O_5(OH)_4$	2%~40%	[14,15,17]
	Illite	$K_{1.5}Al_4(Si_{6.5}Al_{1.5})O_{20}(OH)_4$	1%~30%	[14,15,17]
	montmorillonite	$Na_{0.33}(Al_{1.67}Mg_{0.33})Si_4O_{10}(OH)_2$	<0.1%	[14,15]
	chlorite	$(MgFeAl)_6(AlSi)_4O_{10}(OH)_8$	<0.1%	[14,15]
carbonate	calcite	$CaCO_3$	0.3%~25%	[14–16,18]
	dolomite	$CaMg(CO_3)_2$	<0.5%	[14,15]
	siderite	$FeCO_3$	<1%	[14,15]
	ankerite	$(Ca,Mg,Fe)CO_3$	<5.3%	[14,15]
silicate	quartz	SiO_2	2%~30%	[14,15,18]
oxide	hematite	Fe_2O_3	0.5%~9.5%	[14–16]
sulfide	pyrite	FeS_2	0.5%~7.5%	[14,15,18]
sulfate	gypsum	$CaSO_4 \cdot 2H_2O$	<0.8%	[14,15]
phosphate	apatite	$Ca_5F(PO_4)_3$	<0.8%	[14,15]

Clay minerals are the most common and important mineral constituents of coal, and are formed by coal-forming plants during metamorphism or through weathering of fine rock fragments in a sedimentary environment [14]. Clay minerals are usually filled in cell cavities or dispersed in inertinites, pores, cleats and fractures [19,20]. Studies have shown that the composition and content of clay minerals in coal are related to the sedimentary environment and the degree of metamorphism [19,21–25]. Firstly, the coal-forming environment promotes the mutual transformation of different clay mineral components into coal. The distribution of kaolinite, the main component of the clay minerals, in coal seams is significantly affected by coal seam thermal contact metamorphism. This metamorphism promotes the transformation of kaolinite into clay minerals such as illite and chlorite [21]. Secondly, the degree of coal's metamorphism will affect the content of clay minerals in coal. Zhang et al. [22] determined the contents of clay minerals in coals with different degrees of metamorphism using scanning electron microscope and found that the contents of clay minerals in high rank coals ($R_{o,\,max} > 2.0\%$) were higher than those in the low rank coals ($R_{o,\,max} < 0.5\%$). In 2006, Susilawati et al. [23] studied the overall mineralogical evolution from lignite to anthracite in an Indonesian coal mining area. The results showed that, with the increase in coal's metamorphism, the main mineral of kaolinite in low rank coal was gradually replaced by illite/montmorillonite mixed layer, sodium mica or chlorite. The results showed that the above mineralogical evolution originated from the coal seam thermal contact metamorphism during the coal-forming process. Yang et al. [21] pointed out that when the temperature of the geological environment at which the minerals were formed was $\leq$150 °C, the clay minerals in coal were mainly kaolinite and montmorillonite. At 150–250 °C, the clay minerals were mainly illite and chlorite. The formation temperature of illite was $\geq$137 °C, and that of anthracite was 150–220 °C. Therefore, it can be inferred that anthracite usually coexists with illite because of their formation temperatures [21]. Thirdly, there is an "associated" phenomenon of different clay minerals in coal. Dai et al. [24] found that chlorite in Zhaotong coal (Late Permian) in Yunnan (China) usually formed a copolymer with kaolinite and was filled in the pore structure of vitrinite and inertinite in the coal. Daniels et al. [25] found that the occurrence of authigenic illite in Pennsylvania

anthracite was accompanied by pyrophyllite, chlorite, mixed chlorite/montmorillonite layers and mixed illite/montmorillonite layers.

Carbonate minerals in coal mainly include calcite, dolomite, ankerite and siderite. Some coals contain high magnesium dolomite, rhodochrosite, smithsonite and strontite. To date, the distribution of carbonate minerals in coal mainly includes the following four aspects. First of all, the carbonate minerals in coal are generally the authigenic minerals, whose genesis is mainly related to the igneous rocks invading the coal seams and the accompanying gas and liquid substances rich in CO_2, whereas these minerals exist in the form of coal pores and fracture fillers [19,26]. Secondly, the forms of occurrence of different carbonate minerals in coal are different. Calcite mainly exists in the form of massive clastic, cryptocrystalline, xenomorphic and permeable crystals, whereas dolomite mainly exists in the form of massive cryptocrystalline, allomorphic and permeable crystals [20]. Thirdly, the formation of carbonate minerals in coal depends on the intrusion of existing minerals and mineralized solutions during the peat formation stage and the penetration of mineralized solutions in the coalification stage. Finally, the distribution of carbonate minerals in coal is closely related to other minerals in coal, such as sulfide minerals and quartz. Greb [27] and Raymond [28] found that carbonate minerals (calcite, dolomite and siderite) will form spherical mineralized peat particles with a particle size of about 300 mm with pyrite. Kortenski [20] confirmed that siderite in coal can interact with contemporaneous pyrite crystals, and pointed out that there is a correlation between the formation conditions of carbonate and sulfide. According to studies by Dai [24] and Hower [29], different types of carbonate minerals and non-carbonate facies may occur together in specific fractures and pores of coal seams.

2.2.2. Mineral Transformation in the Oxidation Zone (900–1450 °C)

Oxygen and carbon undergo a multi-phase reaction to generate a lot of heat in the oxidation zone. Therefore, there is a higher temperature in the oxidation zone than that in the reduction zone, which is a significant factor in the phase transformation of minerals in the oxidation zone.

It was found that quartz, anorthite and mullite were the main mineral components of the residue in the oxidation zone of UCG, whereas anorthite was the characteristic product of UCG [30]. Under the distribution and conversion of elements, the content of acid oxides (SiO_2 and Al_2O_3) is generally higher than that of alkaline oxides (CaO and MgO) [31]. The contents of SiO_2, Al_2O_3, CaO and residual carbon in the gasification residue were relatively high. Segregation of SiO_2 and Al_2O_3 also occurred in the oxidation zone of metakaolinite, whereas the activity of Si reached the highest at 1100 °C [32]. At a higher temperature (1100 °C), the materials formed by the segregation of metakaolinite reacted to form mullite, which is a special product in the oxidation zone. With the temperature exceeding 1200 °C, amorphous SiO_2 was crystallized under the action of segregation to form cristobalite. The crystal structure of silicon bearing illite was destroyed and transformed into an amorphous structure at a higher temperature (1093 °C). Furthermore, at 1100 °C, all characteristic diffraction peaks of illite disappeared, which was transformed into mullite crystals [33]. Montmorillonite was transformed into cristobalite and mullite at 1200 °C [34]. In addition, CaO and CO_2 can generate $CaCO_3$ under high-temperature conditions [30]. Tao et al. [35] used Raman spectroscopy to detect the phase of dolomite under high-temperature conditions. It was found that when the temperature exceeded 1100 °C, dolomite changed into calcite and cristobalite. Feldspar minerals such as potassium feldspar, albite and anorthite can also be decomposed at 950–1100 °C [36].

2.2.3. Mineral Transformation in the Reduction Zone (600–900 °C)

During the transition from oxidation to reduction zone, free oxygen was exhausted. Compared with the dry distillation zone, the reduction zone had a higher temperature and the material was prone to endothermic reaction. The residue in the reduction zone was

mainly represented by the expansion, fragmentation and transformation of the material phase of coal.

The migration of major elements such as C, H, N and S changed and these elements were distributed in the reduction zone during the progression of UCG. Other elements such as Al, Si, Ca and O were also transformed and distributed, which mainly came from kaolinite, montmorillonite, illite, quartz, calcite and dolomite. Wei et al. [32] studied the phase transition of kaolinite. The results showed that, at 850 °C, metakaolinite had a phase transition, which was manifested by the segregation of SiO_2. Meanwhile, the structural state of aluminum did not change significantly. When the temperature reached 950 °C, metakaolinite was segregated to form Al_2O_3-γ and the activity of Al reached the highest at 900 °C. Li et al. [33] studied the phase transition of illite at high temperatures, and the experimental results showed that illite was destroyed and transformed into an amorphous structure at 1093 °C. The structure of montmorillonite changed to amorphous structure at 906 °C [34]. Chlorite is quite different from kaolinite, illite, montmorillonite and other minerals; thus, the decomposition products at 900–1000 °C are significantly different, and mainly include magnesium spinel, magnesium oxide and ferric oxide [37]. The phase of carbonate minerals such as calcite, dolomite and siderite also changed significantly. Wang et al. [38] studied the change in phase of dolomite marble under high-temperature conditions, and the results showed that dolomite mineral grains developed smooth and wavy extinction (dislocation climb) and deformed double crystals within the temperature range of 800–1000 °C. Meanwhile, a large number of fine recrystallized grains developed along the grain boundary.

Pyrite, calcined gypsum and anhydrite also underwent phase transformation at higher temperatures. Pyrite transformed into hematite at higher temperature. Gypsum calcine and anhydrite were converted into anhydrite, whereas anhydrite was decomposed under high-temperature conditions to generate calcium oxide and sulfur oxide.

2.2.4. Mineral Transformation in the Dry Distillation Zone (200–600 °C)

In the process of UCG, coal cracking, shrinkage and the removal of mineral water mainly occurred in the dry distillation zone. The minerals of UCG residue were mainly the clay minerals. Kaolinite underwent dehydroxylation at 450–500 °C. When the temperature was higher than 500 °C, the crystal structure of kaolinite was destroyed, and the crystals were transformed into amorphous metakaolinite, with lower flexural strength and higher activity [39]. Li et al. [33] showed that the illite clay mineral containing potassium lost free water at 100–400 °C, whereas hydroxyl was removed at 500–700 °C. Ward [40] found that montmorillonite was relatively rare in coal. Moreover, montmorillonite was related to alteration of volcanic ash. Montmorillonite was dehydrated compared with illite at 126–139 °C. Zhao et al. [37] found that the rare chlorite mineral contains iron, manganese or magnesium as compared to other minerals, so the substance was relatively stable and the pyrolysis products were also very different. Carbonate minerals such as calcite, dolomite and siderite with symbiotic relationship underwent phase transformation under the action of high temperature. Wang et al. [38] studied the change in the phase of dolomite marble under high-temperature conditions. The results showed that the microstructure of dolomite changed at 250 °C, which was mainly characterized by the development of sudden wave extinction. When the temperature reached 500~700 °C, dolomite marble began to develop deformed twin crystals during deformation and shear slip occurred along the twin planes. Meanwhile, the migration of twin boundaries was strengthened. Shao et al. [36] studied the phase change of siderite at high temperatures, and the results showed that the siderite decomposed at 600 °C, forming magnetite. The decomposition temperature of calcite was higher, so there was more calcite in the dry distillation zone. Sulfide and sulfate minerals, such as pyrite and gypsum, also underwent phase transformation at the higher temperature. Gypsum was mainly dehydrated in the dry distillation zone and transformed into gypsum and anhydrite.

3. Pore Structure of the Samples

There are many methods for studying the pore characteristics. The current research methods mainly include the liquid intrusion method and the optical observation method. Liquid intrusion methods mainly include the mercury intrusion method, the low-temperature nitrogen adsorption method and the CO_2 adsorption method. Optical observation methods mainly include optical microscopy, electron microscopy, small-angle X-ray scattering and nuclear magnetic resonance.

The nitrogen adsorption/desorption isotherm and pore size distribution curve of the residues from the three reaction zones of UCG are shown in Figure 4. The results showed that the residue (reduction coal) in the reduction zone had the largest specific surface area and volume for the pores, followed by the residue (dry distillation coal) in the dry distillation zone. The residue (slag) in the oxidation zone had the smallest specific surface area and volume for the pores. Ma et al. showed that the UCG residues in the reduction zone had a specific surface area and volume of up to 54.36 m^2/g and 0.031 cm^3/g, respectively [13]. The residue in the dry distillation zone had a specific surface area and volume of 15.65 m^2/g and 0.014 cm^3/g, respectively. The values for the specific surface area and volume of the oxidation residue were the smallest. The residues in the "three reaction zones" contained certain micropores and mesopores [13,41].

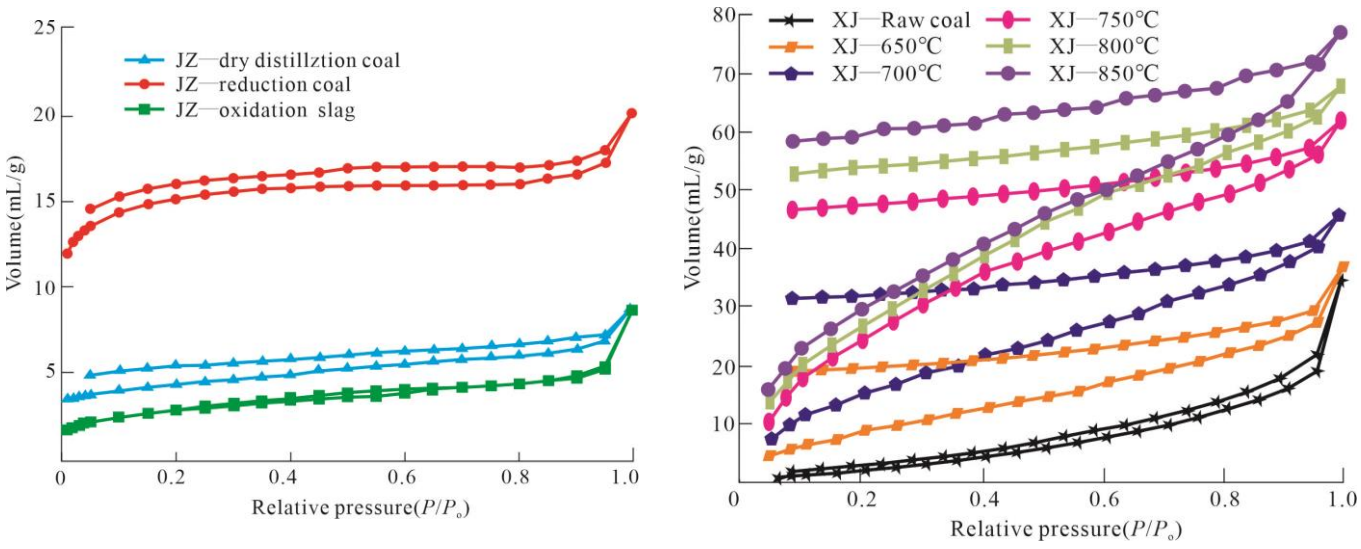

(**a**) (**b**)

Figure 4. N_2 adsorption/desperation isotherms of the samples: (**a**) samples collected from the three reaction zones; (**b**) samples at different temperatures of heat carrier (Adapted from [13,41]). JZ—Jiaozuo coal; XJ—Xinjiang coal.

The pore structures of the residues from the three reaction zones of UCG were significantly different. The temperature in the oxidation zone was the highest, due to which most of the organic matter of the coal was burnt out, and the inorganic minerals were fused and sintered to form a large number of pores, with relatively smaller specific surface areas and volume for pores. After the pyrolysis, in the coal of the reduction zone, the carbon atoms were consumed, which not only expanded the original pyrolysis pores, but also generated some new micropores in the original pores, resulting in a relatively developed porous structure and larger specific surface area. The reduction coal pores were developed, and they had the largest specific surface area and volume.

Previous studies showed that the surface morphology and pore structure of coal changed during the UCG process, and that there were some pores that formed when the volatiles were released quickly, thus providing diffusion channels for the reaction medium, reaction products, and the migration of gases after the UCG process [13,41]. The residues at different final temperatures of heat carrier with the magnification of 1000 times are

shown in Figure 5. The results showed that the surface of the raw coal was relatively flat and only a few cavities could be seen on it. Nevertheless, the residues at different final temperatures were full of pores with different sizes, indicating that the porous structure of the reduced coal was more developed than that in the raw coal and the oxidation slag. Moreover, with the increase in the temperature of heat carrier, the aperture became larger and the surfaces became rougher. The apertures of new pores were much larger than the original pores [13,41].

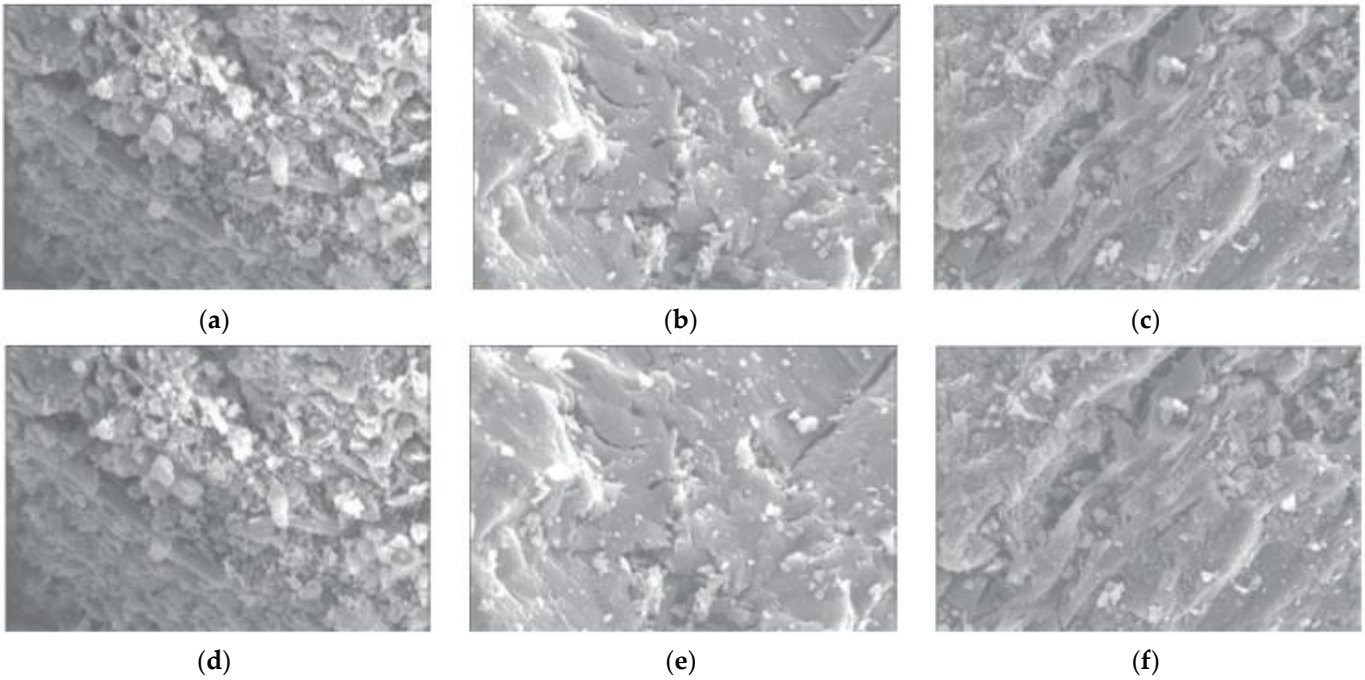

Figure 5. SEM of XJ raw coal and the residues at different temperatures of heat carrier and the magnification at 1000 times: (**a**) raw coal; (**b**) the residue derived from pyrolysis by heat carrier at the final temperature of 650 °C; (**c**) the residue derived from pyrolysis by heat carrier at the final temperature of 700 °C; (**d**) the residue derived from pyrolysis by heat carrier at the final temperature of 750 °C; (**e**) the residue derived from pyrolysis by heat carrier at the final temperature of 800 °C; (**f**) the residue derived from pyrolysis by heat carrier at the final temperature of 850 °C (adapted from [41]).

4. CO_2 Sequestration in the UCG Space

After the UCG of coal seams, the UCG space becomes a good place for CO_2 sequestration. As mentioned above, after the gasification of underground coal seams, the oxidation residues, cavities, reduction residues, and the dry distillation residues were formed around the UCG channel. Moreover, the physical and chemical properties of the residues in the three reaction zones were significantly different due to different reaction environments in the three reaction zones. Due to this reason, CO_2 sequestration in the UCG space included CO_2 mineralization, high-pressure tank, and CO_2 adsorption on the residues and the coal (Figure 6). When CO_2 was injected into the UCG space, a high-pressure tank was formed in the cavities as a natural gas reservoir. Then, CO_2 migrated through the fractures and connecting pores into the UCG slag, UCG reduction residue, dry distillation coal, and raw coal. Finally, the CO_2 was adsorbed in the pores to achieve CO_2 storage.

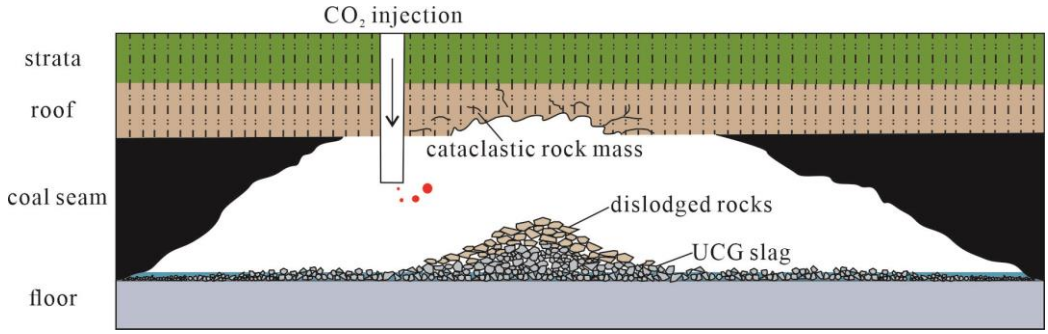

Figure 6. Schematic diagram of CO_2 sequestration in the UCG space.

4.1. CO_2 Mineralization

Because the mineral compositions and occurrence states are different in the three reaction zones after the UCG, the mineralization reaction of CO_2 in the three gasification zones is significantly different as well. Previous studies showed that CO_2 reacts with carbonate, clay and other minerals under water solution condition according to Equations (1)–(5) [42–47].

$$CaCO_3(s) + H^+ \overset{H_2O}{\longleftrightarrow} Ca^{2+} + HCO_3^- \quad (1)$$

$$CaCO_3(s) + CO_2 + H_2O \overset{H_2O}{\longleftrightarrow} Ca^{2+} + 2HCO_3^- \quad (2)$$

$$CaCO_3(s) + H_2O \overset{H_2O}{\longleftrightarrow} Ca^{2+} + HCO_3^- + OH^- \quad (3)$$

$$Al_2Si_3O_5(OH)_4(s) + 6CO_2 + 5H_2O \leftrightarrow 2Al^{3+} + 2H_4SiO_4 + 6HCO_3^- \quad (4)$$

$$K_{0.6}Mg_{2.5}Al_{2.3}Si_{0.6}(OH)_2(s) + H_2O + 0.25CO_2 \leftrightarrow 0.6KAl_2Si_3O_{10}(OH)_2(s) + 0.25Al_2Si_2O_5(OH)_4(s) + 1.2SiO_2 + 0.25Mg(CO_3)_2 \quad (5)$$

In the dry distillation zone, the minerals in the UCG residues are mainly the dehydrated minerals. Therefore, the chemical reaction between CO_2 and minerals is similar to those in the raw coal.

In the oxidation zone, the minerals in the UCG residues are mainly the acidic oxides and the alkaline oxides. CO_2 cannot react with the acidic oxides and, therefore, reacts with the alkaline oxides to achieve carbon sequestration. The reaction of CO_2 with alkaline oxides is shown in Figure 7 and can be represented by Equations (6)–(8).

$$CaO + CO_2 \xrightarrow{H_2O} CaCO_3 \quad (6)$$

$$MgO + CO_2 \xrightarrow{H_2O} MgCO_3 \quad (7)$$

$$FeO + CO_2 \xrightarrow{H_2O} FeCO_3 \quad (8)$$

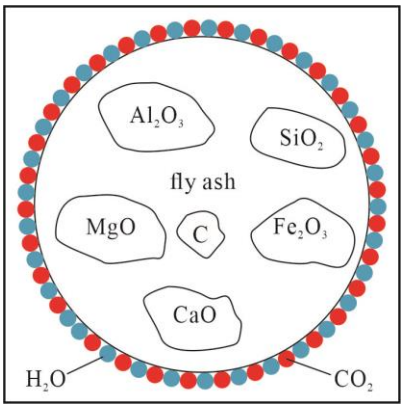

Figure 7. Schematic of the CO_2 reaction with alkaline oxides.

4.2. CO_2 Adsorption

As mentioned above, the UCG residues in the reduction and dry distillation zones contain a large amount of porous carbon media, which provides volumes for CO_2 sequestration in the UCG space. After the UCG, in the oxidation zone, the content of carbon in the UCG slag is very low due to combustion. In the reduction zone, the carbon content of the reduction coal is reduced, and the porosity increases. Meanwhile, in the dry distillation zone, the pore structure changes due to the pyrolysis of heated coal. Therefore, CO_2 can be sequestrated in its adsorbed state in the reduction and dry distillation zones.

Previous studies showed that the gas adsorption capacity on porous carbon media had a normal correlation to the specific surface area of pores [48,49]. This means that the larger the specific surface area of pores, the stronger the gas adsorption and the greater the CO_2 sequestration potential. Therefore, the dry distillation and the reduction zones can sequester more CO_2, which is useful for not only helping obtain the carbon quicker but also contributing towards achieving carbon neutrality.

5. Conclusions

In this study, the results from previous investigations on the physicochemical properties of UCG residues are summarized. In terms of material composition, the residue in the oxidation zone mainly consists of acidic and alkaline oxides, and contains a small amount of residual carbon. The residue in the reduction zone mainly consists of the reduced coal and a small amount of thermally decomposed minerals. The residue mainly consists of pyrolysis coal and heated dehydrated minerals due to the baking of UCG. The UCG increases the porous-specific surface area of the residue in the reduction and dry distillation zones, and reduces the porous-specific surface area of the residue in the oxidation zone.

With the backdrop of carbon neutralization, the UCG space is a good place for CO_2 sequestration. The cavity due to UCG can sequester CO_2 as a high-pressure tank in a natural gas reservoir. The minerals in the gasification residues are easy to carbonate with CO_2 to achieve carbon sequestration, especially for alkaline minerals. As a porous medium, carbon in the residue can adsorb more CO_2 to achieve carbon sequestration.

At present, there are still some limitations in the research of CO_2 sequestration. (1) At present, the research on CO_2 sequestration by UCG cavity is essentially in the theoretical stage. The feasibility of using UCG cavities for CO_2 storage has been demonstrated at the theoretical level. However, the actual operation is affected by geological environment such as temperature and pressure; thus, whether it is suitable for large-scale CO_2 storage needs further test verification. (2) The commercialization of CO_2 sequestration is not yet realized. Whether the benefits obtained from the storage of CO_2 by UCG cavity can offset the costs consumed in the storage process, and therefore whether it has commercial value, needs to be further verified.

Author Contributions: Writing—original draft preparation, R.C., F.L. and Y.B.; writing—review and editing, R.C., Y.B., F.C., T.D. and G.T.; supervision, R.C. and F.C. All authors have read and agreed to the published version of the manuscript.

Funding: The research was funded by the Fundamental Research Funds for the Central Universities (2019XKQYMS24).

Institutional Review Board Statement: Not applicable.

Informed Consent Statement: Not applicable.

Data Availability Statement: Not applicable.

Conflicts of Interest: The authors declare no conflict of interest.

References

1. BP Group. BP Energy Outlook, 2019 [EB/OL]. Available online: https://www.bp.com/content/dam/bp/business-sites/en/global/corporate/pdfs/energy-economics/energy-outlook/bp-energy-outlook-2019.pdf (accessed on 16 February 2019).
2. Zou, C.N.; Xue, H.Q.; Xiong, B.; Zhang, G.S.; Pan, S.Q.; Jia, C.Y.; Wang, Y.; Ma, F.; Sun, Q.; Guan, C.X.; et al. Connotation, innovation and vision of "carbon neutral". *Nat. Gas Ind.* **2021**, *41*, 46–57.
3. Chen, F.; Yu, H.C.; Bian, Z.F.; Yin, D.Y. How to handle the crisis of coal industry in China under the vision of carbon neutrality. *J. China Coal Soc.* **2021**, *46*, 1808–1820.
4. Xie, H.P.; Ren, S.H.; Xie, Y.C.; Jiao, X.M. Development opportunities of the coal industry towards the goal of carbon neutrality. *J. China Coal Soc.* **2021**, *46*, 1808–1820.
5. BP Group. BP Statistical Reviews of World Energy, 2018 [EB/OL]. Available online: https://www.bp.com/en/global/corporate/media/reports-and-publications.html (accessed on 22 October 2018).
6. State Council of the PRC. Several Opinions on Promoting the Coordinated and Stable Development of Natural Gas [EB/OL]. Available online: http://www.gov.cn/zhengce/content/2018-09/05/content_5319419.htm (accessed on 5 September 2018).
7. Klimenko, A.Y. Early ideas in underground coal gasification and their evolution. *Energies* **2009**, *2*, 456–476. [CrossRef]
8. Evgeny, S.; Arvind, V. Underground coal gasification: A brief review of current status. *Ind. Eng. Chem. Res.* **2009**, *48*, 7865–7875.
9. Qin, Y.; Wang, Z.; Han, L. Geological problems in underground coal gasification. *J. China Coal Soc.* **2019**, *44*, 2516–2530.
10. Yang, F.; Duan, Z.H.; Ma, D.M.; Tian, T.; Fu, D.L.; He, D. New development of coal gasification technology. *Sci. Technol. Rev.* **2020**, *38*, 71–85.
11. Liu, S.Q.; Qi, C.; Jiang, Z.; Zhang, Y.J.; Niu, M.F.; Li, Y.Y.; Dai, S.F.; Finkelman, R.B. Mineralogy and geochemistry of ash and slag from coal gasification in China: A review. *Int. Geol. Rev.* **2018**, *60*, 717–735. [CrossRef]
12. Wang, Z. *Establishment of Mass and Energy Balance Model in UCG Process Based on Three Zones Distribution*; China University of Mining and Technology: Beijing, China, 2016.
13. Ma, A.L.; Chen, L.J.; Xu, B. Study on physicochemical properties of "three zone" residues during underground coal gasification. *Coal Sci. Technol.* **2019**, *47*, 217–223.
14. Ward, C.R. Analysis, origin and significance of mineral matter in coal: An updated review. *Int. J. Coal Geol.* **2016**, *165*, 1–27. [CrossRef]
15. Ward, C.R. Analysis and significance of mineral matter in coal seams. *Int. J. Coal Geol.* **2002**, *50*, 135–168. [CrossRef]
16. Yu, X.H.; Sun, P.; Zhang, J.Y.; Tian, C.; Gong, B.G.; Chen, G.; Zhao, Y.C.; Zheng, C.G. Quantitative investigations on mineral matter and distributions of trace elements in Shengfu coal. *J. China Coal Soc.* **2015**, *40*, 2683–2689.
17. Rajabzadeh, M.A.; Ghorbani, Z.; Keshavarzib, B. Chemistry, mineralogy and distribution of selected trace-elements in the Parvadeh coals, Tabas, Iran. *Fuel* **2016**, *174*, 216–224. [CrossRef]
18. Zhuang, X.G.; Querol, X.; Zeng, R.S.; Xu, W.D.; Alastuey, A.; Lopez-Soler, A.; Plana, F. Mineralogy and geochemistry of coal from the Liupanshui mining district, Guizhou, South China. *Int. J. Coal Geol.* **2000**, *45*, 21–37. [CrossRef]
19. Permana, A.K.; Ward, C.R.; Li, Z.S.; Gurba, L.W. Distribution and origin of minerals in high-rank coals of the South Walker Creek area, Bowen Basin, Australia. *Int. J. Coal Geol.* **2013**, *116*, 185–207. [CrossRef]
20. Kortenski, J. Carbonate minerals in Bulgarian coals with different degrees of coalification. *Int. J. Coal Geol.* **1992**, *20*, 225–242. [CrossRef]
21. Yang, Q.; Pan, Z.G.; Weng, C.M.; Su, Y.C.; Wang, Z.P. *Discussion on Metamorphic Characteristics and Geological Factors of Permian Carboniferous Coal in North China*; Geological Publishing House: Beijing, China, 1988; p. 81.
22. Zhang, P.A.; Yuan, J.; Wen, C.; Luo, G.Q.; Yu, D.X.; Yao, H. CCSEM investigation on the mineral properties of six Chinese typical steam coals. *J. China Coal Soc.* **2016**, *41*, 2326–2331.
23. Susilawati, R.; Ward, C.R. Metamorphism of mineral matter in coal from the Bukit Asam deposit, south Sumatra, Indonesia. *Int. J. Coal Geol.* **2006**, *68*, 171–195. [CrossRef]
24. Dai, S.F.; Chou, C.L. Occurrence and origin of minerals in a chamosite-bearing coal of Late Permian age, Zhaotong, Yunnan, China. *Am. Mineral.* **2007**, *92*, 1253–1261. [CrossRef]

25. Daniels, E.J.; Aleaner, S.P. Clay mineral authigenesis in coal and shale from the Anthracite region, Pennsylvania. *Am. Mineral.* **1990**, *75*, 825–839.
26. Zhao, L.; Ward, C.R.; French, D.; Graham, I.T. Mineralogy of the volcanic-influenced Great Northern coal seam in the Sydney Basin, Australia. *Int. J. Coal Geol.* **2012**, *94* (Suppl. S1), 94–110. [CrossRef]
27. Greb, S.F.; Eble, C.F.; Chestnud, D.R.; Phillips, T.L.; Hower, J.C. An in-situ occurrence of coal balls in the Amburgy coal bed, Pikeville Formation (Duckmantian), central Appalachian Basin, USA. *Palaios* **1999**, *14*, 432–450. [CrossRef]
28. Raymond, A.; Guillemette, R.; Jones, C.P.; Ahr, W.M. Carbonate petrology and geochemistry of Pennsylvanian coal balls from the Kalo Formation of Iowa. *Int. J. Coal Geol.* **2012**, *94* (Suppl. S1), 137–149. [CrossRef]
29. Hower, J.C.; Williams, D.A.; Eble, C.F.; Sakulpitakphon, T.; Moecher, D.P. Brecciated and mineralized coals in Union County, Western Kentucky coal field. *Int. J. Coal Geol.* **2001**, *47*, 223–234. [CrossRef]
30. Liu, S.; Qi, C.; Zhang, S.; Deng, Y.P. Minerals in the ash and slag from oxygen—Enriched underground. *Minerals* **2016**, *6*, 27–42. [CrossRef]
31. Zhao, Y.B.; Wu, H.; Cai, X.L.; Zhuo, J.D.; Lai, S.Y.; Liu, H.G.; Jing, Y.H.; Yuan, W. Basic Characteristics of coal gasification residual. *Clean Coal Technol.* **2015**, *21*, 110–113, 74.
32. Wei, C.D.; Yang, D.; Li, Y.; Mikuni, A. Influence of temperature on phase transformation of calcined kaolinite and Si, Al activity. *Acta Mineral. Sin.* **2005**, *25*, 197–202.
33. Li, G.H.; Jiang, T.; Fang, X.H.; Qui, G.Z. Thermochemical activation of silicon in illite and its removal. *Met. Mine* **2004**, *5*, 18–21.
34. Liu, Y.Q.; Lv, X.J.; Qiu, J. Theories and comparison of several methods for measuring layer charge density of montmorillonites. *Sci. Online* **2008**, *3*, 288–292.
35. Tao, Y.C.; Hao, Z.Y.; Jia, P.; Lu, C.H. Raman spectrum analysis of pyrophillite and dolomite by HP-HT. *Diam. Abras. Eng.* **2003**, *138*, 61–64.
36. Shao, J.B.; Shao, X.X.; Wang, Z.N. Influence of mineral composition in coal on properties of fly ash. *Coal Process. Compr. Util.* **1996**, 37–41.
37. Zhao, L.; Dai, S.F.; Zhang, Y.; Wang, X.B.; Li, D.; Yan-feng, L.; Zhu, X.W.; Sun, Y.Y.; Ma, Y.W. Mineral abundances of high-alumina fly ash from the Jungar Power Plant, Inner Mongolia, China. *J. China Coal Soc.* **2008**, *33*, 1168–1172.
38. Wang, H.; Song, M.S.; Li, J.F.; Zhang, G.N.; Shao, T.B.; Wang, X.N.; Wang, S.M. Experimental study on deformation property of Yunnan dolomite marble under high-temperature and high-pressure conditions. *Geotecton. Metallog.* **2020**, *44*, 852–983.
39. Kuang, J.Z.; Qiu, T.S.; Shi, F. Effect of heat treatment on structure transformation and activities of kaolinite. *Chin. J. Nonferrous Met.* **2012**, *22*, 258–264.
40. Ward, C.R. Review of mineral matter in coal. *Aust. Coal Geol.* **1986**, *6*, 87–110.
41. Zhou, G.L.; Wu, J.J.; Miao, Z.Y.; Hu, X.L.; Li, X.; Shi, X.; Cai, Z.D.; Shang, Y.K. Effects of process parameters on pore structure of semi-coke prepared by solid heat carrier with dry distillation. *Int. J. Min. Sci. Technol.* **2013**, *23*, 423–427. [CrossRef]
42. Du, Y.; Sang, S.X.; Wang, W.F.; Liu, S.Q.; Wang, T.; Fang, H.H. Experimental study of the reactions of supercritical CO_2 and minerals in high-rank coal under formation conditions. *Energy Fuels* **2018**, *32*, 1115–1125. [CrossRef]
43. Chen, R.; Qin, Y. Fluid-solid coupling between supercritical CO_2 and minerals in coal and geological significances. *Coal Sci. Technol.* **2012**, *40*, 17–21.
44. Harvey, O.R.; Qafoku, N.P.; Cantrell, K.J.; Lee, G.; Amonette, J.E.; Brown, C.F. Geochemical implications of gas leakage associated with geologic CO_2 storage—A qualitative review. *Environ. Sci. Technol.* **2013**, *47*, 23–36. [CrossRef]
45. Manning, D.A.C.; Renforth, P. Passive sequestration of atmospheric CO_2 through coupled plant-mineral reactions in urban soils. *Environ. Sci. Technol.* **2013**, *47*, 135–141. [CrossRef]
46. Jorat, M.E.; Kraavi, K.E.; Manning, D.A.C. Removal of atmospheric CO_2 by engineered soils in infrastructure projects. *J. Environ. Manag.* **2022**, *314*, 115016. [CrossRef] [PubMed]
47. Washbourne, C.L.; Lopez-Capel, E.; Renforth, P.; Ascough, P.L.; Manning, D.A. Rapid removal of atmospheric CO_2 by urban soils. *Environ. Sci. Technol.* **2015**, *49*, 5434–5440. [CrossRef] [PubMed]
48. Zhong, L.W. Adsorptive capacity of coals and its affecting factors. *Earth Sci.-J. China Univ. Geosci.* **2004**, *29*, 327–332, 368.
49. Chen, R.; Qin, Y.; Wei, C.T. Differences in pore structures and adsorptivity between raw and two-step-solvent extracted vitrains. *Nat. Gas Geosci.* **2014**, *25*, 1103–1110.

Disclaimer/Publisher's Note: The statements, opinions and data contained in all publications are solely those of the individual author(s) and contributor(s) and not of MDPI and/or the editor(s). MDPI and/or the editor(s) disclaim responsibility for any injury to people or property resulting from any ideas, methods, instructions or products referred to in the content.